

Coexistence-curve diameter and critical density of xenon

Ulrike Narger and David A. Balzarini

Physics Department, University of British Columbia, Vancouver, British Columbia, Canada V6T 2A6

(Received 16 April 1990)

We have measured the coexistence-curve diameter and the critical density of xenon with very high accuracy, using an optical technique which allows us to obtain data of the refractive index and the density in the same experiment. Contrary to theoretical predictions, we observe no deviations from rectilinear diameter in Xe, to an accuracy of at least 0.05% of the critical density. This finding may give information about the dominant many-body interactions between the fluid atoms. The critical refractive index was determined as the limiting value of the coexistence-curve diameter as the temperature approaches T_c . This method has the advantage of being entirely self-contained and not depending on other data for the evaluation of ρ_c . Two different samples of Xe were studied. One of them yields $n_c = 1.13774 \pm 0.00010$ for the critical refractive index and $\rho_c = 1.1160 \pm 0.0017$ g/cm³ for the critical density, and the other yields $n_c = 1.13743 \pm 0.00012$ and $\rho_c = 1.1147 \pm 0.0017$ g/cm³. These results agree within experimental error and are the most accurate measurements of the critical density of Xe to date.

I. INTRODUCTION

We have carried out measurements of the refractive index and density of xenon in the critical region in an effort to determine the critical density with as high an accuracy as possible. Two different samples were studied, and thus the reproducibility of the critical density for samples from different suppliers (and therefore probably containing different impurities) could be investigated.

The refractive index and the density are related by the Lorentz-Lorenz relation

$$\mathcal{L} = \frac{1}{\rho} \frac{n^2 - 1}{n^2 + 2}, \quad (1)$$

where \mathcal{L} , the Lorentz-Lorenz function, is a weak function of density. If \mathcal{L} is known, the density can be determined from a measurement of the refractive index.

In a pure fluid, the order parameter $\Delta\rho^*$ is proportional to the density difference between liquid and vapor phases, i.e.,

$$\Delta\rho^* = \frac{\rho_l - \rho_v}{2\rho_c}. \quad (2)$$

Scaling theories predict that upon approach to the critical point, $\Delta\rho^*$ should obey a power law in the reduced temperature $t = (T_c - T)/T_c$, with an exponent β . The exponent β is expected to be universal, i.e., its value depends only on the dimensionality of the system, the number of components of the order parameter, and the range of the microscopic interactions. Pure fluids belong to the same universality class as the three-dimensional Ising model.¹ Values of β have been calculated by both high-temperature series expansions^{2,3} and ϵ expansions,^{4,5} giving β between 0.325 and 0.327. The pure scaling law is exact only very close to the critical point for pure fluids in a temperature interval $t < 10^{-5}$. For larger reduced

temperatures, corrections due to the irrelevant scaling fields have to be taken into account,^{1,6} so that the order parameter should be described by

$$\Delta\rho^* = B_0 t^\beta (1 + B_1 t^\Delta + B_2 t^{2\Delta} + \dots), \quad (3)$$

where B_0 , B_1 , and B_2 are (nonuniversal) amplitudes and Δ is the universal correction to the scaling exponent. Δ has been calculated to lie between 0.49 and 0.54.^{2,4,7}

The average of liquid and vapor densities defines the coexistence-curve diameter ρ_d of the coexistence curve, which, close to the critical point, is expected¹ to behave like

$$\rho_d = (\rho_l + \rho_v)/2 = \rho_c + A_{1-\alpha} t^{1-\alpha} + A_1 t + \dots \quad (4)$$

Here, the term linear in t corresponds to the "law of rectilinear diameter."⁸ Recently, a microscopic theory^{9,10} has interpreted this deviation of the diameter from a straight line as resulting from many-body interactions between the fluid molecules. If the dominant contribution to the many-body forces are assumed to be due to dipole-induced-dipole interactions of the Axilrod-Teller type,¹¹ it is found that both A_1 and $A_{1-\alpha}$ are proportional to the critical polarizability product $\alpha_p \rho_c$,¹⁰ where α_p is the polarizability and ρ_c is the critical density. Since the polarizability product of Xe is unusually high,¹² one would, in the framework of this theory, expect Xe to exhibit a large slope of the diameter A_1 , as well as a deviation from rectilinear diameter $A_{1-\alpha}$, which is more pronounced than that found in other nonpolar fluids.⁹ Measurements on the coexistence-curve diameter of Xe thus give valuable information on the validity of this theory.

Our objective in these experiments was to measure \mathcal{L} , $\Delta\rho^*$, and ρ_d , and thus to get an estimate of the critical density ρ_c . There have been several previous measurements of the critical density. Some of them use P - V - T data to determine the critical parameters.¹³⁻¹⁶ Other experiments use optical techniques to measure the critical

refractive index.¹⁷⁻¹⁹ These optical experiments also rely on P - V - T data, however, as they measure refractive indices as a function of cell pressures and have to use an equation of state to relate the pressures to densities.

Our experiment had the advantage that it uses no previous data, but was entirely self-contained. We determined the critical density in the following way: (i) Measurement of the Lorentz-Lorenz function \mathcal{L} , i.e., determination of the density ρ as a function of refractive index n along the coexistence curve, as defined by Eq. (1). (ii) Determination of the critical refractive index n_c as the limiting value of the average of liquid and vapor refractive indices as the temperature approaches T_c :

$$n_c = \lim_{T \rightarrow T_c} \frac{n_l(T) + n_v(T)}{2}. \quad (5)$$

The value of T_c was obtained from a fit to the order parameter $\Delta\rho^*$ as given in Eq. (3). Knowing n_c , the critical density ρ_c was then calculated from Eq. (1). (iii) As a check on consistency, we calculated the densities ρ_l, ρ_v from our measured refractive index data n_l, n_v , using Eq. (1). We then fitted the mean density ρ_d to Eq. (4) and used the intercept ($t=0$) to extract ρ_c .

As slight changes of composition can influence the critical temperature and pressure of a substance quite dramatically,²⁰ a small error in the measurement of ρ_c does not necessarily imply a high accuracy of the result. In order to be of general use, the result must be reproducible for different samples of Xe. In an effort to verify the reproducibility of our value of ρ_c , we studied two samples from two different batches of Xe.

The remainder of this paper is organized as follows: Section II describes the experimental technique. Section III presents the results of the Lorentz-Lorenz measurements and the order parameter and coexistence-curve-diameter data. Finally, Sec. IV discusses the results and compares our values with the literature. A detailed error calculation is given in the Appendix.

II. EXPERIMENTAL TECHNIQUE

Experiments were performed on two different samples of xenon. One of them (sample No. 1) was purchased from Matheson Gas Products and rated 99.995% pure by the supplier. We had obtained it just prior to the experiments discussed below. Thus no long-term contamination in the gas cylinder took place while the gas was in our possession. The other one (sample No. 2) had been obtained from Professor R. Gammon at the University of Maryland.

Figure 1 shows the experimental setup used for the experiments. The sample cell had an aluminum body with a prism-shaped head.²¹ It was filled with a given mass of Xe and placed in a thermostat which controlled the temperature to within 0.5 mK. A collimated laser beam passing through the prism is deflected by an angle which depends on the index of refraction of the fluid in the cell. The beam is reflected into an autocollimating telescope (Davison, model D275) by a micrometer-driven mirror (Lansing Research Corp., model 10.253). By adjusting

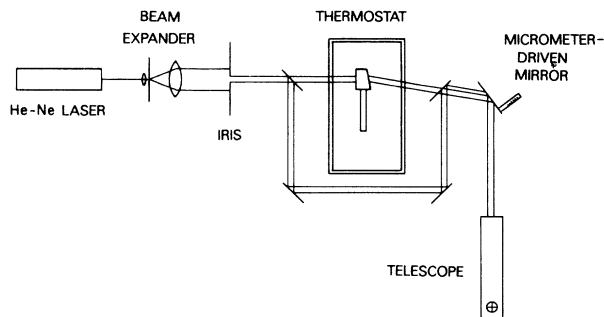


FIG. 1. Optical setup of the prism-cell experiment.

the mirror, the refraction angle can be measured. A reference beam passing around the cell is used to monitor the stability of the alignment.

In order to obtain precise measurements, a series of calibrations had to be carried out. The Appendix describes these calibrations and shows the effects of the various uncertainties on the resulting value of the critical density.

The measurement of the Lorentz-Lorenz function proceeded as follows: The cell, containing a given mass of fluid, was cooled into the two-phase region where the fluid phase separates into liquid and vapor. Since the system is on the coexistence curve, the density, and thus the refractive index, of each phase is temperature dependent. The temperature of the cell was then raised until the system passed from the two-phase into the one-phase region where the refractive index is independent of temperature. The refractive index was measured just above the coexistence curve in the one-phase region. By repeating this procedure for different overall densities, the Lorentz-Lorenz function, and thus the relationship between density and refractive index along the coexistence curve, could be extracted.

When the overall density in the cell was close to the critical value, measurements of the refractive indices along the coexistence curve were carried out: In the two-phase region, the refractive indices of both liquid and vapor phases, n_l and n_v , were recorded as a function of temperature. From these data, the order parameter and coexistence-curve diameter could be determined.

Close to the critical point, the large compressibility of the fluid causes the density profile to be strongly curved. This gravitational effect smears the extended laser beam traversing the cell close to T_c and thus limits the accuracy with which the deflection angles can be determined. In our prism experiment, we cannot approach the critical point closer than 10^{-4} in reduced temperature before gravitational rounding begins to affect the accuracy of the data.^{21,22}

III. RESULTS

A. Lorentz-Lorenz function

The Lorentz-Lorenz function \mathcal{L} , as defined in Eq. (1), provides the link between the refractive index and the

TABLE I. Results of a quadratic fit to the Lorentz-Lorenz data of two Xe samples. The first fit is a quadratic fit centered around $\rho_c = 0.0085 \text{ mol/cm}^3$. $\mathcal{L}_c(\text{fit})$ is the critical value of \mathcal{L} , averaged over various fits. $\langle \mathcal{L} \rangle$ is the average of \mathcal{L} measurements in the density interval $0.88\rho_c < \rho < 1.12\rho_c$.

	\mathcal{L}_0 (cm^3/mol)	\mathcal{L}_1 (cm^6/mol^2)	\mathcal{L}_2 (cm^9/mol^3)	$\mathcal{L}(\text{fit})$ (cm^3/mol)	$\langle \mathcal{L} \rangle$ (cm^3/mol)
Sample No. 1	10.410	24.80	-1459	10.515 ± 0.001	
Sample No. 2	10.387	27.78	-1634	10.505 ± 0.002	
Sample No. 1	10.413	25.28	-1569	10.515 ± 0.001	10.510 ± 0.008
Sample No. 2	10.382	26.19	-1377	10.505 ± 0.003	10.504 ± 0.006

density of a fluid. The data were fitted to a second-order polynomial in the density ρ :

$$\mathcal{L}(\rho) = \mathcal{L}_0 + \mathcal{L}_1\rho + \mathcal{L}_2\rho^2. \quad (6)$$

For a first set of fits, the fitted parabola was assumed to be symmetric around the critical density ($\rho_c = 0.0085 \text{ mol/cm}^3$). Table I summarizes result of these fits in the density interval $0.3\rho_c < \rho < 1.4\rho_c$. Results of fits treating the position of the maximum of the parabola as a free parameter are also given in Table I, together with the results of the critical value $\mathcal{L}_c = \mathcal{L}(\rho_c)$. When the location of the maximum of the fit to the Lorentz-Lorenz function is treated as a free parameter, it is shifted to a lower density than ρ_c in sample No. 1, whereas it is shifted to a

higher density than ρ_c in sample No. 2. No systematic shift is thus observable.

Because of the scatter of the data points, the error in $\mathcal{L}_c(\text{fit})$, obtained from a fit to the data, is considerably smaller than $\langle \mathcal{L}_c \rangle$, which was calculated by averaging the Lorentz-Lorenz values in the density interval $0.88\rho_c < \rho < 1.12\rho_c$.

Figure 2 shows the Lorentz-Lorenz data of both samples, together with the curves corresponding to the fit parameters given in Table I (treating the maximum of the parabola as a free parameter). Note that the discrepancy between the \mathcal{L}_c values of the two data sets is less than 0.1%. Within the accuracy of our measurements, we observe no anomaly of \mathcal{L} close to the critical point, in agreement with other researchers.^{17,19}

From the Lorentz-Lorenz data, the electronic (optical) polarizability α_p can be determined using²³

$$\lim_{\rho \rightarrow 0} \mathcal{L}(\rho) = \frac{4\pi\alpha_p}{3} N_A, \quad (7)$$

where N_A is Avogadro's number. For Xe, we find $\alpha_p = 4.12 \pm 0.01 \text{ \AA}^3$.

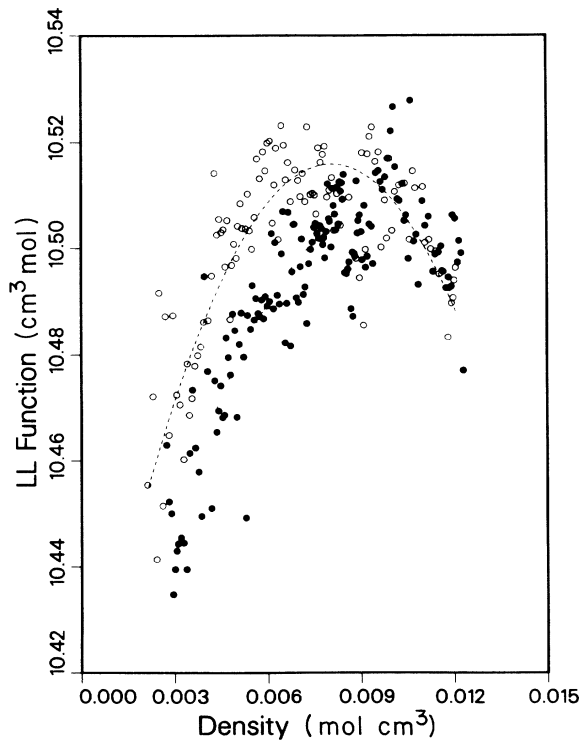


FIG. 2. Lorentz-Lorenz data of sample No. 1 (\circ) and sample No. 2 (\bullet). The curves correspond to quadratic fits to the data.

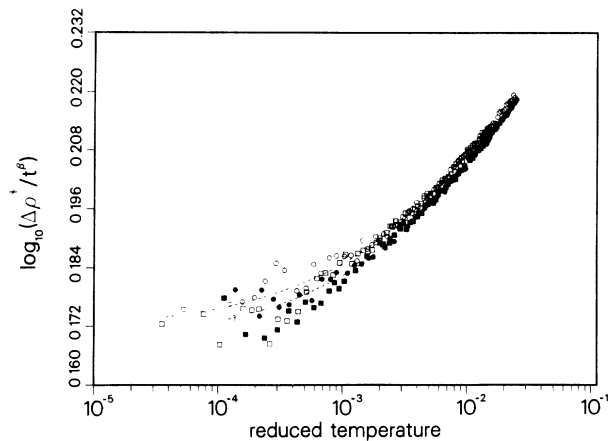


FIG. 3. log-log plot of the order parameter data of Xe: Open symbols correspond to data taken on sample No. 1, solid symbols to data taken on sample No. 2. The dashed curves are fits with two correction to scaling terms and keeping $\beta = 0.327$ and $\Delta = 0.5$ fixed.

TABLE II. Results of fits to the coexistence curve of Xe in the reduced temperature interval $10^{-4} < t < 3 \times 10^{-2}$. For these fits, the exponents $\beta=0.327$ and $\Delta=0.5$ were held fixed.

	B_0	B_1	B_2	T_c [°C]
Sample No. 1	1.479 ± 0.011	1.15 ± 0.19	-2.6 ± 1.0	16.602 ± 0.001
Sample No. 2	1.470 ± 0.010	1.20 ± 0.17	-2.8 ± 1.1	16.639 ± 0.002

B. Determination of the critical temperature

The critical temperature was determined by fitting the coexistence-curve data to a power law in the reduced temperature with corrections to scaling, as given in Eq. (3). Two coexistence-curve runs were performed on each of the samples. Because of gravitational rounding effects, the data are confined to reduced temperatures $t > 5 \times 10^{-5}$, where the critical asymptotic behavior has not yet been reached. Therefore, for fits of the order parameter, the exponents $\beta=0.327$ and $\Delta=0.5$ were held fixed, and the critical temperature and three amplitudes were fitted as free parameters. Figure 3 shows a plot of $\log_{10} \Delta^* \rho / t^\beta$ as a function of reduced temperature t . The fit results are given in Table II. The values of the amplitudes and critical temperature are the averages of several fits to the combined data of the two runs in each sample. The amplitudes of sample Nos. 1 and 2 are seen to agree within error. There is a systematic difference in the values of the critical temperatures, however. Both values of T_c are in good agreement with values found in previous experiments [$T_c=16.64^\circ\text{C}$ (Ref. 24) and $T_c=16.615^\circ\text{C}$ (Ref. 16)]. The difference in critical temperature between sample Nos. 1 and 2 may be due to different impurities present in the two samples. It has been shown that even small contaminations can cause considerable changes in the critical temperature.²⁰ These contaminations seem to have a negligible effect on the values of the amplitudes.

C. Coexistence-curve diameter and critical density

In order to determine the critical refractive density ρ_c , the behavior of the coexistence-curve diameter, $\rho_d = (\rho_l + \rho_v)/2$, as a function of the reduced temperature was studied. For each data set, the critical temperature was held fixed at the value found from the coexistence-curve fits.

Figure 4 shows a plot of the diameter data of Sample Nos. 1 and 2 as a function of reduced temperature. In all cases, the data exhibit no significant deviations from straight lines. We thus do not observe any singularity of the coexistence-curve diameter. Table III gives the diameter-fit results. The first part of the table shows the parameters obtained from a straight-line fit to the data with reduced temperatures $t > 8 \times 10^{-3}$. For each sample, the data of the two runs were fitted together. The error is a measure of the difference between the two runs. The second part of the table gives results of fits treating A_1 and $A_{1-\alpha}$ as free parameters. The exponent α was kept constant at $\alpha=0.11$. When only a linear term is fitted ($A_{1-\alpha}=0$), the values found for A_1 agree very well with the slopes of the straight-line fits in the outer tem-

perature range $t > 8 \times 10^{-3}$. This indicates that there are indeed no systematic deviations from rectilinear diameter close to the critical point. Fitting both A_1 and $A_{1-\alpha}$ as free parameters does not give useful results, as indicated by the large errors.

The limiting value of the diameter ρ_d as $t \rightarrow 0$ determines the critical density ρ_c . We calculated the value of ρ_c for our samples by averaging the ρ_c values obtained in the various diameter fits. The results are the following:

$$\begin{aligned} \text{sample No. 1: } \rho_c &= 0.008\,496(4) \text{ mol/cm}^3 \\ &= 1.1156(5) \text{ g/cm}^3, \end{aligned}$$

$$\begin{aligned} \text{sample No. 2: } \rho_c &= 0.008\,489(4) \text{ mol/cm}^3 \\ &= 1.1139(5) \text{ g/cm}^3. \end{aligned}$$

For an evaluation of the uncertainty in the value of ρ_c due to systematic errors, it turns out to be easier to extract the limiting value of n_c as $t \rightarrow 0$ of the refractive-index diameter $(n_l + n_v)/2$, which is directly accessible experimentally, and to calculate ρ_c using the Lorentz-Lorenz relation. The error calculation is presented in the Appendix. The results are the following:

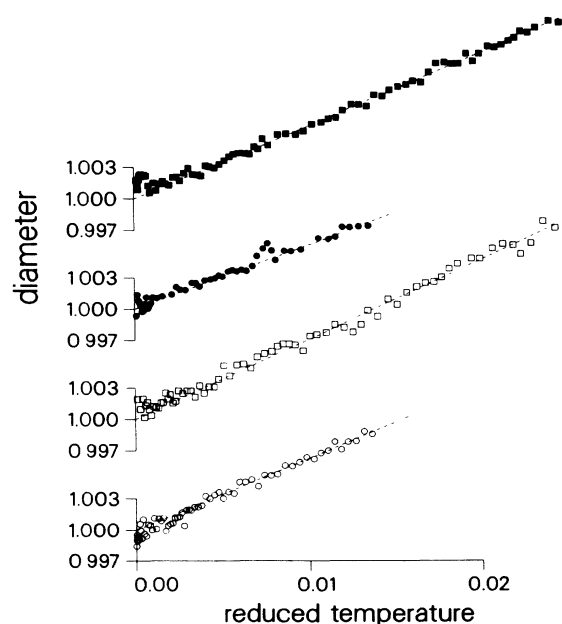


FIG. 4. Coexistence-curve diameter ρ_d of Xe as a function of t for four experimental runs. Open symbols correspond to data on sample No. 1, solid symbols to data on sample No. 2.

TABLE III. Fit results of the coexistence-curve diameter of Xe. Parameters in parentheses were kept fixed for the fit. The exponent α was held fixed at $\alpha=0.11$.

	A_1	$A_{1-\alpha}$	ρ_c (mol/cm ³)
Outer temperature range ($t > 8 \times 10^{-3}$)			
Sample No. 1	0.70±0.04	(0.0)	0.008 495(4)
Sample No. 2	0.65±0.04	(0.0)	0.008 481(8)
Total temperature range ($10^{-5} < t < 2 \times 10^{-2}$)			
Sample No. 1	0.69±0.02	(0.0)	0.008 497(2)
	(0.0)	0.47±0.02	0.008 492(1)
	1.3±1.0	-0.5±0.3	0.008 502(2)
Sample No. 2	0.66±0.01	(0.0)	0.008 484(7)
	(0.0)	0.43±0.02	0.008 481(6)
	1.4±1.0	-0.5±0.3	0.008 488(8)

sample No. 1: $n_c = 1.1377 \pm 0.0001$,

$$\rho_c = 1.1160 \pm 0.0017 \text{ g/cm}^3,$$

sample No. 2: $n_c = 1.1374 \pm 0.0001$,

$$\rho_c = 1.1147 \pm 0.0017 \text{ g/cm}^3.$$

The small difference of the critical densities found in the two evaluations are well within error.

IV. DISCUSSION AND COMPARISON WITH OTHER EXPERIMENTS

The Lorentz-Lorenz function just above the coexistence curve can be fitted well by a quadratic function of the refractive index. Within the accuracy of our experiment, we observe no critical anomaly in the Lorentz-Lorenz function; nor do we observe any discontinuities in \mathcal{L} . The Lorentz-Lorenz data measured in the two different samples of Xe agree to within 0.1%. Our value of the critical value of $\mathcal{L}(\rho_c) = \mathcal{L}_c = 10.510 \pm 0.005$ cm³/mol agrees well with other experiments which find the Lorentz-Lorenz function to have an average value of $\langle \mathcal{L} \rangle = 10.52 \pm 0.02$ cm³/mol (Ref. 19) and $\langle \mathcal{L} \rangle = 10.53 \pm 0.07$ cm³/mol (Ref. 17) in the density region $0.6\rho_c < \rho < 1.8\rho_c$. We measure the critical index by extrapolation of the refractive-index diameter as $T \rightarrow T_c$ and find $n_c = 1.1377 \pm 0.0001$ for sample No. 1 and $n_c = 1.1374 \pm 0.0001$ for sample No. 2, in excellent agreement with the value of Garside *et al.* who found $n_c = 1.1379 \pm 0.0008$.¹⁸

The critical density is determined from the Lorentz-Lorenz relation at the critical point. Table IV compares our value of ρ_c to other experiments. Our results for \mathcal{L}_c and n_c carry a smaller error than the values of other researchers, and thus our value of ρ_c has a much smaller uncertainty. (For a detailed error evaluation, see the Appendix.) Since our method is entirely self-contained and no outside information was used to determine ρ_c , the value is also probably very accurate.

TABLE IV. Critical density of xenon.

Experimenter	ρ_c
Habgood and Schneider (Ref. 13)	1.099 g/cm ³
Levelt (Ref. 15)	1.091 g/cm ³
Chapman <i>et al.</i> (Ref. 17)	1.1055±0.004 g/cm ³
Garside <i>et al.</i> (Ref. 18)	1.119±0.011 g/cm ³
Baidakov <i>et al.</i> (Ref. 16)	1.1128 g/cm ³
Cornfeld and Carr (Ref. 25)	1.1128±0.0006 g/cm ³
	1.1113±0.0017 g/cm ³
This work	
Sample No. 1	1.1160±0.0017 g/cm ³
Sample No. 2	1.1147±0.0017 g/cm ³

In our data for the coexistence-curve diameter of Xe, we observe no critical deviation from linear diameter, in agreement with other experiments.²⁵ We conclude that any critical-diameter singularity, if present in Xe, is less than 0.05% of ρ_c close to the critical point. Thus we find that the law of rectilinear diameter is obeyed to high precision in Xe. This is in contradiction with the theory of Goldstein *et al.*,⁹ according to which we would expect an anomaly whose magnitude should be proportional to $\alpha_p \rho_c$. For Xe, $\alpha_p \rho_c = 0.021$, larger than in any of the nonpolar gases studied in Ref. 10 which all display critical singularities of the diameter. Thus we would expect the anomaly in Xe to be larger than observed in other fluids. However, there are indications²⁶ that in the Xe system the Axilrod-Teller interactions are not the most important three-body forces. Rather, exchange interactions play a dominant role. These, however, are not taken into account in the theory of Goldstein *et al.* If exchange interactions were to partly cancel the effect of the Axilrod-Teller interactions, this could explain why the theory of Goldstein *et al.* does not correctly predict the diameter anomaly in Xe.

The critical temperature is very sensitive to impurities, leading to large shifts in critical temperature when small impurities are added.²⁰ Even though their critical temperatures vary, the critical densities of sample Nos. 1 and 2 agree very well, indicating that whatever impurities they may have contained, these impurities have a minor impact on the critical density. The close agreement leads us to believe that our value of the critical density is a very good estimate of the critical density of research-purity xenon in general.

ACKNOWLEDGMENTS

We would like to thank E. Derbez for his help in data acquisition and J. R. de Bruyn, R. Gammon, and K. T. Pang for helpful discussions. This research was funded by the National Sciences and Engineering Research Council of Canada.

APPENDIX: ERROR ANALYSIS FOR THE CRITICAL DENSITY

This Appendix describes how the refractive index of a fluid inside the prism cell can be obtained from the re-

fraction angle and presents an error evaluation for the critical density obtained from a prism-cell measurement.

Calculation of refractive index from refraction angle

We assume that the incident beam is incident on the first (straight) window of the prism at right angles. The refracted beam leaves the prism at an angle κ with respect to the incident beam. Figure 5 shows the geometry and defines the angles. All dotted lines correspond to directions parallel to the incident beam. All dot-dashed lines indicate normals to the window faces. n_s , n_a , and n_{Xe} are the refractive indices of sapphire, air, and xenon, respectively. θ_s (θ_t) is the wedge angle of the straight (tilted) window, and θ is the prism angle. Angles α_i are between the beam direction and a surface normal, κ_i are angles between the beam and the direction of the incident beam, and κ is the total (measured) refraction angle. As the wedge angles of the windows θ_s and θ_t are small, we can Taylor expand to obtain

$$\sin\theta_s \approx \theta_s, \quad \sin\theta_t \approx \theta_t, \quad \cos\theta_s \approx \cos\theta_t \approx 1.$$

Using Snell's law for refraction angles, one then obtains the refractive index n_{Xe} as a function of the refraction angle κ , to first order in θ_s and θ_t :

$$n_{Xe} = (n_a / \sin\theta) (\sin(\kappa + \theta) + \theta_t \{ \cos(\kappa + \theta) - [n_s^2 / n_a^2 - \sin^2(\kappa + \theta)]^{1/2} \}) + \theta_s [\sin(\kappa + \theta) \cot\theta - (n_s / n_a) \cos\theta]. \quad (A1)$$

Error estimates

The estimate of errors was essential for judging the accuracy of the critical densities determined in the prism-cell experiments. The following quantities were calibrated with the given accuracy. (i) Systematic errors:

- (1) Prism angle $\theta = 20.525^\circ$, with $\delta\theta = 0.010^\circ$.
- (2) Sapphire window wedges: straight window: $\theta_s = -0.00018$, $\delta\theta_s = 0.00002$, tilted window: $\theta_t = -0.00041$, $\delta\theta_t = 0.00003$.
- (3) Volume of prism cell $V = 12.066 \text{ cm}^3$, $\delta V = 0.003 \text{ cm}^3$.
- (4) Mass of empty prism cell: $M_0 = 179.3995 \text{ g}$, $\delta M_0 = 0.0030 \text{ g}$. Items (1) and (2) limit the accuracy of refractive-index measurements. They lead to errors δn_{pr} , δn_s , and δn_t due to the error in the prism angle θ , and the tilt angles θ_s and θ_t , respectively. Items (3) and (4) limit the accuracy of the density $\rho = M/V$.

(ii) Random errors.

- (1) Mass readings.
- (2) Micrometer reading.
- (3) Temperature reading. These errors produce a random error $\delta\mathcal{L}_c$ in the value of the Lorentz-Lorenz function at the critical point and a statistical error δn_c in the critical refractive index. In our experiments we found that

$$\left[\frac{\delta n_c}{n_c} \right]_{\text{stat}} \approx 1.8 \times 10^{-4}, \quad \left[\frac{\delta\mathcal{L}_c}{\mathcal{L}_c} \right]_{\text{stat}} \approx 2.9 \times 10^{-4}.$$

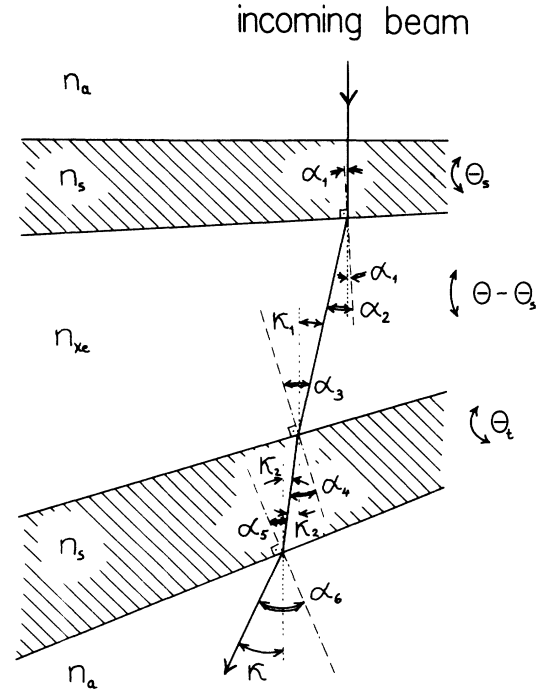


FIG. 5. Refraction geometry of the prism-cell experiment. For an explanation of the symbols, see text.

The total error in the critical density can then be evaluated to be

$$\frac{\delta\rho_c}{\rho_c} = \left[\left[\left[\frac{\delta\mathcal{L}_c}{\mathcal{L}_c} \right]_{\text{stat}} \right]^2 + C^2 \left[\frac{\delta n_c}{n_c} \right]_{\text{tot}}^2 + \left[\frac{\delta\rho_c}{\rho_c} \right]_{\text{sys}}^2 \right]^{1/2} = 1.5 \times 10^{-3}, \quad (A2)$$

where

$$\left[\frac{\delta n_c}{n_c} \right]_{\text{tot}}^2 = \left[\frac{\delta n_c}{n_c} \right]_{\text{stat}}^2 + \left[\frac{\delta n_{pr}}{n_c} \right]^2 + \left[\frac{\delta n_s}{n_c} \right]^2 + \left[\frac{\delta n_t}{n_c} \right]^2$$

and

$$\left[\frac{\delta\rho_c}{\rho_c} \right]_{\text{sys}}^2 = \left[\frac{\delta M}{M} \right]_c^2 + \left[\frac{\delta V}{V} \right]_c^2 \approx 3.4 \times 10^{-4}.$$

The parameter C is obtained from a Taylor expansion of the Lorentz-Lorenz relation around the critical point and is given by

$$C = \frac{6n_c^2}{(n_c^2 + 2)(n_c^2 - 1)}.$$

- ¹M. Ley-Koo and M. S. Green, Phys. Rev. A **23**, 2650 (1981).
- ²M. J. George and J. J. Rehr, Phys. Rev. **53**, 2061 (1977).
- ³J. H. Chen, M. E. Fisher, and B. G. Nickel, Phys. Rev. Lett. **48**, 630 (1982).
- ⁴J. C. LeGuillou and J. Zinn-Justin, Phys. Rev. B **21**, 3976 (1980).
- ⁵B. Nickel and M. Dixon, Phys. Rev. B **26**, 3965 (1982).
- ⁶F. J. Wegner, Phys. Rev. B **5**, 4529 (1972).
- ⁷J. Adler, M. Moshe, and V. Privman, Phys. Rev. B **26**, 3958 (1982).
- ⁸L. Cailletet and E. C. Matthias, R. Hebd. Seanc. Acad. Sci., Paris **102**, 1202 (1886).
- ⁹R. E. Goldstein, A. Parola, N. W. Ashcroft, M. W. Pestak, M. H. W. Chan, J. R. de Bruyn, and D. A. Balzarini, Phys. Rev. Lett. **58**, 41 (1987).
- ¹⁰M. W. Pestak, R. E. Goldstein, M. H. W. Chan, J. R. de Bruyn, D. A. Balzarini, and N. W. Ashcroft, Phys. Rev. B **36**, 599 (1987).
- ¹¹B. M. Axilrod and E. Teller, J. Chem. Phys. **11**, 299 (1943).
- ¹²H. H. Landolt and R. Börnstein, *Zahlenwerte and Tabellen II/1* (Springer-Verlag, Berlin, 1951), p. 346.
- ¹³H. W. Habgood and W. G. Schneider, Can. J. Chem. **32**, 98 (1954).
- ¹⁴A. Michels, T. Wassenaar, and P. Louwerse, Physica **20**, 99 (1954).
- ¹⁵J. M. H. Levelt, Physica **26**, 361 (1960).
- ¹⁶V. G. Baidakov, A. M. Rubshtein, V. R. Pomortsev, and I. J. Sulla, Phys. Lett. A **131**, 119 (1988).
- ¹⁷J. A. Chapman, P. C. Finnimore, and B. L. Smith, Phys. Rev. Lett. **21**, 1306 (1968).
- ¹⁸D. H. Garside, H. V. Molgaard, and B. L. Smith, J. Phys. B **1**, 449 (1968).
- ¹⁹D. Y. Parpia and B. L. Smith, J. Phys. C **4**, 2254 (1971).
- ²⁰J. R. Hastings, J. M. H. Levelt Sengers, and F. W. Balfour, J. Chem. Thermodyn. **12**, 1009 (1980).
- ²¹D. Balzarini and P. Palffy, Can. J. Phys. **52**, 2007 (1974).
- ²²M. R. Moldover, J. V. Sengers, R. W. Gammon, and R. J. Hocken, Rev. Mod. Phys. **51**, 79 (1979).
- ²³H. H. Landolt and R. Börnstein, *Zahlenwerte and Tabellen I/3*, Ref. 12, p. 509ff.
- ²⁴H. Güttinger and D. S. Cannell, Phys. Rev. A **24**, 3188 (1981).
- ²⁵A. B. Cornfeld and H. Y. Carr, Phys. Rev. Lett. **29**, 28 (1972).
- ²⁶E. E. Polymeropoulos, J. Brickmann, L. Jansen, and R. Block, Phys. Rev. A **30**, 1593 (1984).